THE JOURNAL OF BIOLOGICAL CHEMISTRY
Vol. 278, No. 19, Issue of May 9, pp. 17532–17538, 2003
Printed in U.S.A.
© 2003 by The American Society for Biochemistry and Molecular Biology, Inc.

Syntaxin 1A Binds to the Cytoplasmic C Terminus of Kv2.1 to Regulate Channel Gating and Trafficking*

Received for publication, December 23, 2002, and in revised form, February 19, 2003
Published, JBC Papers in Press, March 5, 2003, DOI 10.1074/jbc.M213088200

Yuk M. Leung‡§, Youhou Kang‡, Xiaodong Gao‡, Fuzhen Xia‡, Huanli Xie‡, Laura Sheu‡, Sharon Tsuk¶, Ilana Lotan¶, Robert G. Tsushima‡‖, and Herbert Y. Gaisano‡**

From the ‡Departments of Medicine and Physiology, University of Toronto, Toronto M5S 1A8, Canada and the ¶Departments of Physiology and Pharmacology, Sackler School of Medicine, Tel-Aviv University, Tel-Aviv 69978, Israel

Voltage-gated K^+ (Kv) 2.1 is the dominant Kv channel that controls membrane repolarization in rat islet β-cells and downstream insulin exocytosis. We recently showed that exocytotic SNARE protein SNAP-25 directly binds and modulates rat islet β-cell Kv 2.1 channel protein at the cytoplasmic N terminus. We now show that SNARE protein syntaxin 1A (Syn-1A) binds and modulates rat islet β-cell Kv2.1 at its cytoplasmic C terminus (Kv2.1C). In HEK293 cells overexpressing Kv2.1, we observed identical effects of channel inhibition by dialyzed GST-Syn-1A, which could be blocked by Kv2.1C domain proteins (C1: amino acids 412–633, C2: amino acids 634–853), but not the Kv2.1 cytoplasmic N terminus (amino acids 1–182). This was confirmed by direct binding of GST-Syn-1A to the Kv2.1C1 and C2 domains proteins. These findings are in contrast to our recent report showing that Syn-1A binds and modulates the cytoplasmic N terminus of neuronal Kv1.1 and not by its C terminus. Co-expression of Syn-1A in Kv2.1-expressing HEK293 cells inhibited Kv2.1 surfacing, which caused a reduction of Kv2.1 current density. In addition, Syn-1A caused a slowing of Kv2.1 current activation and reduction in the slope factor of steady-state inactivation, but had no affect on inactivation kinetics or voltage dependence of activation. Taken together, SNAP-25 and Syn-1A mediate secretion not only through its participation in the exocytotic SNARE complex, but also by regulating membrane potential and calcium entry through their interaction with Kv and Ca^{2+} channels. In contrast to Ca^{2+} channels, where these SNARE proteins act on a common synprint site, the SNARE proteins act not only on distinct sites within a Kv channel, but also on distinct sites between different Kv channel families.

In neurons and neuroendocrine cells, depolarization opens voltage-dependent Ca^{2+} channels (VDCC),[1] and the subsequent Ca^{2+} influx triggers exocytosis of neurotransmitters or hormones. Vesicle fusion with the plasma membrane is initiated by the sensing of Ca^{2+} by the vesicle protein synaptotagmin. This is followed by, through yet unclear mechanisms, core complex formation by SNARE (soluble *N*-ethylmaleimide-sensitive factor attachment protein receptors) proteins, which involve another vesicle protein synaptobrevin (vesicle-SNARE) and two plasma membrane SNARE proteins SNAP-25 and syntaxin 1 (target-SNAREs) (1–3). It is proposed that core complex formation brings the two apposing membranes together and liberates the energy required to drive lipid reorientation during fusion (1–3). SNARE proteins have been known to be tethered to various VDCC, and thus such a protein complex may provide rapid release response with SNARE proteins exposed to a high local Ca^{2+} concentration permeating through the VDCCs, which in turn are being modulated by the SNARE proteins (4–8). Because of such an intimate physical and functional coupling, the secretory vesicle-SNARE protein-Ca^{2+} channel complex has been termed excitosome (6). Therefore, besides their participation in membrane fusion, SNARE proteins appear to have a regulatory role on other components (*i.e.* membrane ion channels) of the exocytotic process.

During increased glucose metabolism, a high intracellular ATP to ADP concentration ratio ([ATP]/[ADP]) causes inhibition of pancreatic islet β-cell ATP-sensitive K^+ channels (K_{ATP}) channels, which in turn results in depolarization and consequently insulin release (9). Outward currents carried by voltage-gated K^+ (Kv) channels in β-cells are responsible for repolarization, which results in closure of VDCC and subsequent termination of exocytosis (10–13). The role for these Kv channels in β-cell excitation-secretion coupling is of clinical therapeutic importance, as blocking Kv channels with pharmacological agents can prolong depolarization and enhance Ca^{2+} entry, and thereby sustain insulin secretion in a glucose-dependent manner (14, 15). Although SNARE protein-Ca^{2+} channel interaction has been studied in great detail, little is known about SNARE protein-Kv channel interaction. Recently, using the *Xenopus* oocyte expression system and coimmunoprecipitation experiments, we have shown that SNAP-25 and Syn-1A physically interact with Kv1.1 and Kv2.1 (16–19). Functionally, SNAP-25 inhibits Kv1.1 and Kv2.1 currents, and such inhibition was mediated through binding of SNAP-25 to the Kv1.1

* This work was supported by Grant DK55160 from the National Institutes of Health, the Juvenile Diabetes Research Foundation and the Canadian Diabetes Association (to H. Y. G.) and by Grant MOP 39498 from the Canadian Institutes of Health Research, J. H. Cummings Foundation, and J. P. Bickell Foundation (to R. G. T.), and the Heart and Stroke Foundation of Ontario (NA 5012, to R. G. T. and H. Y. G.). The costs of publication of this article were defrayed in part by the payment of page charges. This article must therefore be hereby marked "*advertisement*" in accordance with 18 U.S.C. Section 1734 solely to indicate this fact.

§ Supported by Fellowship Awards from the Heart and Stroke Foundation of Canada and the Dept. of Medicine (University of Toronto).

‖ Supported by a New Investigator Award from the Heart and Stroke Foundation of Canada. To whom correspondence may be addressed: Medical Sciences Bldg., Rm. 7308, 1 King's College Circle, University of Toronto, Toronto, Ontario M5S 1A8, Canada. Tel.: 416-978-8899; Fax: 416-978-8765; E-mail: r.tsushima@utoronto.ca.

** To whom correspondence may be addressed: Medical Sciences Bldg., Rm. 7226, 1 King's College Circle, University of Toronto, Toronto, Ontario M5S 1A8, Canada. Tel.: 416-978-1526; Fax: 416-978-8765; E-mail: herbert.gaisano@utoronto.ca.

[1] The abbreviations used are: VDCC, voltage-dependent Ca^{2+} channels; Syn-1A, syntaxin 1A; SNAP-25, synaptosome-associated protein of 25 kDa; Kv, voltage-dependent K^+ channels; GST, glutathione *S*-transferase; GFP, green fluorescent protein; SNARE, soluble *N*-ethylmaleimide-sensitive factor attachment protein receptors; FITC, fluorescein isothiocyanate; HEK, human embryonic kidney.

This paper is available on line at http://www.jbc.org

This is an Open Access article under the CC BY license.

and Kv2.1 cytoplasmic N termini (16, 17). We have also shown that Syn-1A has a concentration-dependent biphasic effect on Kv1.1 current amplitudes: at low concentration it enhances current without affecting surface channel expression while at high concentration it decreases current amplitude probably by reducing surface channel expression (18). More recently, we further demonstrated that Syn-1A also binds to the cytoplasmic N terminus of Kv1.1, at the T1A domain and forms a stable complex with G$\beta\gamma$ subunits (19). In this work, we surprisingly found that Syn-1A binds to the cytoplasmic C terminus of islet β-cell Kv2.1 channel protein and modulates channel properties. Syn-1A, when overexpressed, also inhibited Kv2.1 surface expression and reduced Kv2.1 current density in heterologous HEK293 cells. Although SNARE protein interactions with Kv channels follow a similar paradigm as the Ca^{2+} channels, the interacting domains within and between the Kv channel families seem to be distinct in contrast to the highly conserved synprint site (cytoplasmic II-III loop) between the Ca^{2+} channel families (4–6,8).

MATERIALS AND METHODS

Cell Culture and Transfections—HEK293 cells were grown at 37 °C in 5% CO_2 in Dulbecco's modified Eagle's medium supplemented with 10% fetal bovine serum (Invitrogen) and penicillin-streptomycin (100 units/ml, 100 μg/ml) (Invitrogen). The cells were transiently transfected with GFP and Kv2.1 with or without Syn-1A using LipofectAMINE 2000 (Invitrogen). Two days after transfection, cells were trypsinized and placed in 35-mm dishes for voltage-clamp experiments. Transfected cells were identified by visualization of the fluorescence of the co-expressed GFPs.

Islet Isolation—Rat pancreatic islets were isolated by collagenase digestion as described previously (17). Islets were dispersed to single cells by treatment with 0.015% trypsin (Invitrogen) in Ca^{2+}- and Mg^{2+}-free phosphate-buffered saline. Islet cells were plated on glass coverslips in 35-mm dishes and cultured in low glucose Roswell Park Memorial Institute medium (2.5 mM glucose) supplemented with 7.5% fetal bovine serum, 0.25% HEPES (Sigma-Aldrich Canada Ltd.), and 100 units/ml penicillin G sodium, 100 μg/ml streptomycin sulfate (Invitrogen). Islet cells were cultured for 2 days before electrophysiological recordings.

DNA Constructs and Generation of GST Fusion Proteins—The vectors pcDNA3-Kv2.1, pcDNA3-Syntaxin 2, and pcDNA3-Syntaxin 1A were generously provided by Dr. R. Joho (University of Texas, Southwestern Medical Center, Dallas, TX) and Richard Scheller (Stanford University, Palo Alto, CA). The coding sequences corresponding to N-terminal region (1–182) of Kv 2.1 were amplified by polymerase chain reaction (PCR) and cloned into pGEX-5X-1 expression vector (Amersham Biosciences Inc.) for generation of GST fusion proteins. The primers used for PCR were 5′-ATGACGAAGCATGGCTCGC (sense) and 5′-CACCGACGAGTTGGGCT (antisense). The plasmids pGEX-4T-1-Kv2.1-C1 (the region corresponding to amino acids 412–633) and pGEX-4T-1-Kv2.1-C2 (the region corresponding to amino acids 634–853) were similarly generated. These constructs were verified by DNA sequencing. pGEX-4T-1-syntaxin-1A (wild type) is a gift from Dr. W. Trimble (The Hospital for Sick Children, Toronto, Ontario, Canada). GST fusion protein expression and purification were performed following the manufacturer's instructions. Syn-1A was obtained by cleavage of GST-Syn-1A with thrombin (Sigma).

In Vitro Binding Studies—GST (as a control) and GST-Kv2.1-N or -C1 or -C2 (500 pmol of protein each) were bound to glutathione-agarose beads and incubated with thrombin-cleaved Syn-1A (500 pmol of protein) in 200 μl of binding buffer (25 mM HEPES pH 7.4, 50 mM NaCl, 0.1% gelatin, 0.1% Triton X-100, 0.1% bovine serum albumin, and 0.2% β -mercaptoethanol) at 4 °C for 2 h with constant agitation. The beads were then washed two times with washing buffer containing 20 mM HEPES pH 7.4, 150 mM KOAc, 1 mM EDTA, 1 mM $MgCl_2$, 5% glycerol, and 0.1% Triton X-100. The samples were then separated on 15% SDS-PAGE, transferred to nitrocellulose membrane (Millipore, Bedford, MA), and identified with specific primary antibody against Syn-1A (1:2000) (Sigma).

Electrophysiology—HEK293 cells were voltage-clamped in the whole-cell configuration (20) using an EPC-9 amplifier and Pulse software (HEKA Electronik, Lambrecht, Germany) as we previously described (7, 8). Recording pipettes were pulled from 1.5-mm borosilicate glass capillary tubes (World Precision Instruments, Inc., Sarasota, FL) using a programmable micropipette puller (Sutter Instrument). Pipettes were then fire-polished and tip resistances ranged from 1.5–3 MΩ (for HEK cells) or 2.5–4 MΩ (for β-cells) when filled with intracellular solution, containing (in mM): 140 KCl, 1 $MgCl_2$, 1 EGTA, 10 HEPES, and 5 MgATP (pH 7.25 adjusted with KOH). Bath solution contained (mM): 140 NaCl, 4 KCl, 1 $MgCl_2$, 2 $CaCl_2$, 10 HEPES (pH 7.3 adjusted with NaOH). After a whole-cell configuration was established, membrane potential was held at −70 mV and outward currents were triggered with depolarizing voltage pulses (+70 mV, 250 ms). Steady-state outward currents was determined as the mean current in the final 95–99% of the 250-ms pulse. All experiments were performed at room temperature (22–24 °C). Data for voltage dependence of activation and steady-state inactivation were fit by the Boltzmann equation: $I/I_{max} = 1/\{1 + \exp[(V - V_{1/2})/k]\}$, where $V_{1/2}$ is the half-maximal activation potential (for voltage dependence of activation) or the half-maximal inactivation potential (for steady-state inactivation), and k the slope factor. Results are presented as means ± S.E. Unpaired Student's t test was employed, and $p < 0.05$ was considered statistically significant.

Confocal Immunofluorescence Microscopy—Laser confocal immunofluorescence microscopy was performed as described previously (17). Transfected HEK cells were fixed with 100% methanol on 3-aminopropyltriethoxysilane-treated glass slides. The slides were then incubated at 4 °C overnight with primary antibodies, including mouse monoclonal anti-Kv2.1 (1:100) (Upstate Biotechnology Inc., Lake Placid, NY), rabbit anti-syntaxin-1 (Calbiochem, San Diego, CA) (1:100) and rabbit anti-syntaxin-2 (1:200, kindly provided by Dr. V. Olkkonen, National Public Health Institute, Helsinki, Finland). The slides were rinsed four times with phosphate-buffered saline containing 0.1% saponin and treated with secondary antibodies (FITC sheep anti-mouse IgG 1:500 or Texas Red-labeled goat anti-rabbit IgG 1:250) for 1 h. Next, they were incubated with 0.1% p-phenylenediamine (ICN, Cleveland, OH) in glycerol and examined using a laser scanning confocal imaging system (LSM-410; Carl Zeiss, Thornwood, NY). FITC signal was visualized by excitation at a wavelength of 488 nm and emitted fluorescence was measured through a 515- to 540-nm bandpass filter. Texas Red signal was visualized by an excitation wavelength of 568 nm and emitted fluorescence was detected through a 590-nm long-pass filter.

Cell Surface Biotinylation—Two days after transfection HEK293 cells were washed and harvested in phosphate-buffered saline. The cells were further washed with borate buffer (154 mM NaCl, 7.2 mM KCl, 1.8 mM $CaCl_2$, 10 mM boric acid, pH 9.0) and then incubated in 5 ml of Sulfo-NHS-SS-Biotin (Pierce Biotechnology Inc.) (0.5 mg/ml) in borate buffer at 4 °C for 30 min. After washing three times with ice-cold quenching buffer (192 mM glycine, 25 mM Tris, pH 8.3), cells were solubilized on ice in 500 μl of immunoprecipitation buffer (1% deoxycholic acid, 1% Triton X-100, 0.1% SDS, 150 mM NaCl, 1 mM EDTA, 10 mM Tris-Cl, pH 7.5) containing a mixture of protease inhibitors (Roche Applied Science). The cell lysate was centrifuged for 20 min at 16,000 × g, and the supernatant was retained. 50 μl of immobilized streptavidin resin (Pierce) (50% slurry in phosphate-buffered saline containing 2 mM NaN_3) was added to the supernatant, which was then incubated overnight at 4 °C with gentle rocking. Samples were centrifuged for 2 min at 8,000 × g, and the resin was washed five times with immunoprecipitaton buffer. The protein was eluted from the resin by the addition of SDS-PAGE sample buffer containing 5% 2-mercaptoethanol and incubation at 65 °C for 5 min. The samples were analyzed for Kv2.1 expression by Western blotting using anti-Kv2.1 (1:1000, Alomone Labs, Jerusalem, Israel). Integrated density of the bands was determined using a commercial software (Scion Image Beta 4.02; Scion Corporation, Frederick, MD).

RESULTS

Syn-1A Inhibits Rat Islet β-Cell Kv2.1 Activity—We had previously shown that Kv2.1 channels account for ~60% of the outward current in rat islet β-cells (15, 17, 21), making this cell an excellent model to examine the effects of Syn-1A on this channel. Fig. 1*A* shows the current-voltage relationships of outward K^+ currents in rat islet β-cells after an 8-min dialysis with various fusion proteins. For clarity, the results are presented as bar graphs at two positive voltages, which triggered outward currents (+10 and +60 mV) (Fig. 1, *B* and *C*). GST alone was used as a control that by itself did not cause any significant effect on β-cell outward K^+ currents (data not shown). GST-Syn-1A (1 μM) caused a 26 and 22% reduction ($p < 0.05$) in current density at +10 and +60 mV, respectively.

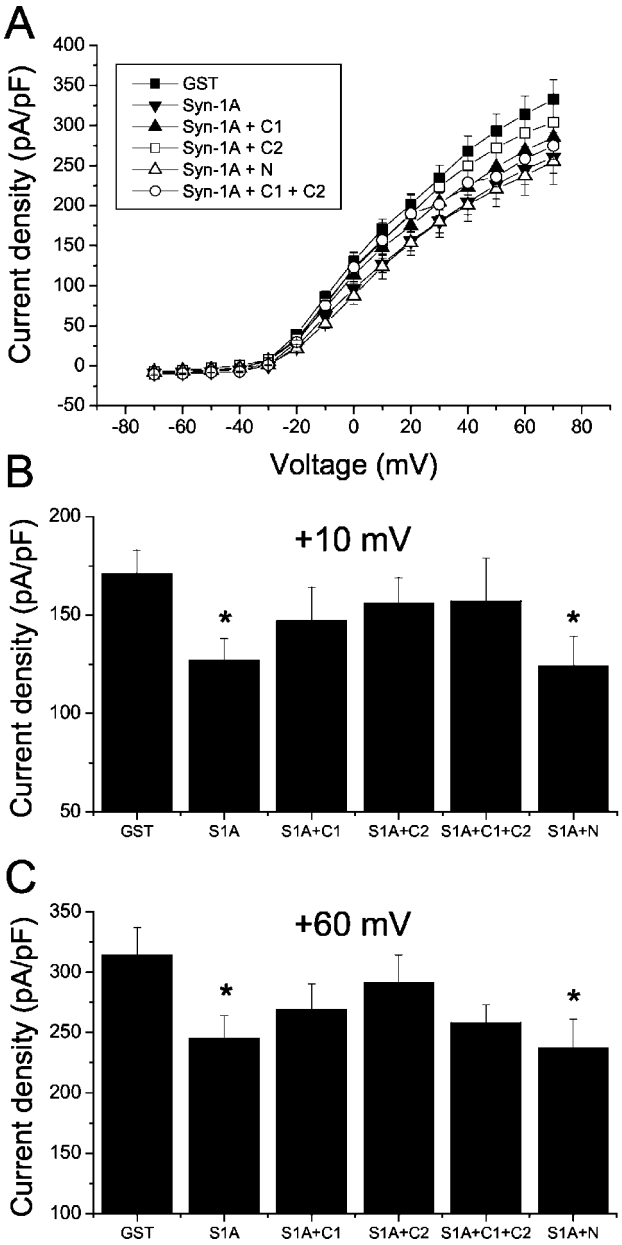

FIG. 1. **Inhibition of β-cell K^+ currents by dialysis of Syn-1A fusion protein was attenuated by Kv2.1 C-terminal fragments but not affected by Kv2.1 N terminus.** *A*, after dialysis of Syn-1A ($n = 9$), GST ($n = 8$), Syn-1A + C1 ($n = 5$), Syn-1A + C2 ($n = 10$), Syn-1A + C1 + C2 ($n = 4$), or Syn-1A + N terminus ($n = 5$) (all at 1 μM) into the β-cell for 8 min, the current-voltage relationship of β-cell outward K^+ currents was studied using the protocol in which the cell was held at −70 mV and was then given depolarizing pulses (250 ms) at 10 mV increments. Currents were normalized by cell capacitance to yield current densities. *B* and *C*, for clarity, the current densities for each treatment group are presented as *bar graphs* at two voltages, +10 and +60 mV. *, $p < 0.05$ when compared with the GST control.

We then examined whether this is mediated via the cytoplasmic N terminus (amino acids 1–182) as we had reported with Kv1.1 (16) or with the cytoplasmic C terminus (amino acids 411–853). Since the cytoplasmic C terminus of Kv2.1 is quite large and difficult to generate the recombinant protein, we generated two smaller sections of this protein, C1 (412–633) and C2 (634–853). Surprisingly, we found that co-dialysis with C1 and/or C2 prevented Syn-1A from inhibiting the Kv2.1 currents, with C2 being more effective than C1, whereas the cytoplasmic Kv2.1 N terminus had no effect on Syn-1A actions. These data suggest that Syn-1A inhibited β-cell Kv2.1 currents by interacting with the Kv2.1 C terminus.

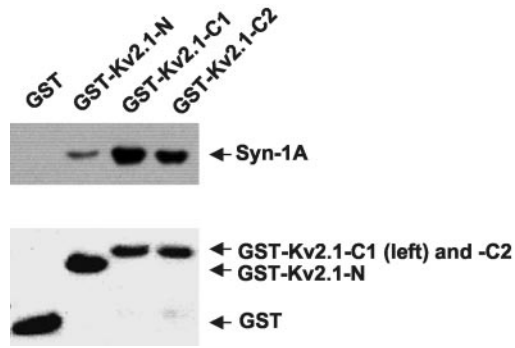

FIG. 2. **Binding of Syn-1A to Kv2.1 C- and N-terminal fragments.** Binding assays were performed as described under "Materials and Methods." *Top panel*, using a specific anti-Syn-1A antibody, Syn-1A bound strongly with Kv2.1 C1 and C2. Kv2.1 N terminus bound only weakly with Syn-1A while GST did not bind Syn-1A at all. *Bottom panel*, Ponseau S staining of the blot to demonstrate the amount of GST protein loaded.

We next investigated whether the interactions between Syn-1A and the Kv2.1 C1 and C2 domains are direct by direct protein binding studies and functional studies using a heterologous expression model system (*i.e.* HEK293), which has little if any endogenous expression of these proteins (22).

Syn-1A Inhibits Kv2.1 Channel Activity by Directly Acting on Its Cytoplasmic C Terminus—Binding assay and electrophysiological data from our previous reports (16, 17) suggest that SNAP-25 inhibits Kv1.1 and Kv2.1 current by binding to the cytoplasmic N terminus. We have also shown that Syn-1A binds to the N terminus of Kv1.1 (19). We therefore examined if Syn-1A bound to the cytoplasmic N or C terminus of Kv2.1 by performing the binding assay with recombinant proteins (Fig. 2). Syn-1A (Fig. 2, *top panel*) bound very strongly with C1 and less so with C2. Syn-1A bound only weakly with the N terminus. As a negative control, GST did not bind to Syn-1A at all. Fig. 2, *bottom panel*, shows a Ponseau S staining of the blot, which demonstrates the equal protein loading of the C1 and C2 proteins, whereas the N-terminal protein and GST were loaded somewhat more but nonetheless showed little and no binding to Syn-1A, respectively. Immunostaining of this blot with anti-GST antibodies confirmed the presence of these proteins (data not shown).

As shown in Fig. 3, dialyzing Syn-1A-GST fusion protein through the recording pipette into Kv2.1-transfected cell caused a reduction (14.4 ± 5.0%; $p < 0.05$) of Kv2.1 current after 6–8 min. This reduction could be abolished by co-dialysis with C1 or C2. Again, similar to the results with rat islet β-cell Kv2.1 channels, C2 was more effective than C1 in blocking the effects of the dialyzed GST-Syn-1A. However, Kv2.1 N terminus was completely ineffective in preventing such reduction. These data indicate that Syn-1A inhibited Kv2.1 currents by a direct interaction with the cytoplasmic C terminus.

Syn-1A Reduces Kv2.1 Channel Surface Expression and Current Density—Dialysis of the Syn-1A might either interact with a cytosolic protein and may not be specifically targeted to the plasma membrane where the Kv2.1 channel is situated. This could be circumvented by overexpressing Syn-1A, which would be appropriately targeted to the plasma membrane compartment (7). Furthermore, Syn-1A has been shown to not only affect Kv1.1 channel function but also affected surface expression of Kv.1.1 in *Xenopus* oocytes (18). As shown in Fig. 4*A*, expression of Syn-1A drastically reduced Kv2.1 current density (0.21 ± 0.05 nA/pF compared with Kv2.1 alone 0.99 ± 0.18 nA/pF; $p < 0.05$). The reduction in Kv2.1 current density in the presence of syntaxin-2 (Syn-2) was small and insignificant.

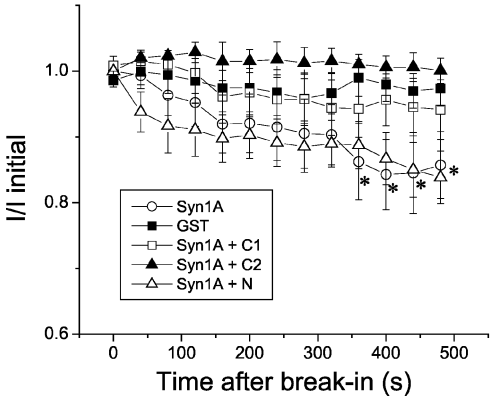

FIG. 3. **Reduction of HEK293 cell Kv2.1 current by dialysis of Syn-1A fusion protein was abolished by Kv2.1 C-terminal fragments but not affected by Kv2.1 N terminus.** The effects of dialysis of Syn-1A (n = 15), GST (n = 12), Syn-1A + C1 (n = 9), Syn-1A + C2 (n = 4) or Syn-1A + N terminus (n = 10) (all at 10 nM) on Kv2.1 current magnitude were tested by giving a +70 mV pulse (250 ms) from a holding potential of −70 mV every 40 s after membrane break-in. Currents are normalized to the initial current magnitude immediately after membrane rupture. *, $p < 0.05$ when compared with GST alone.

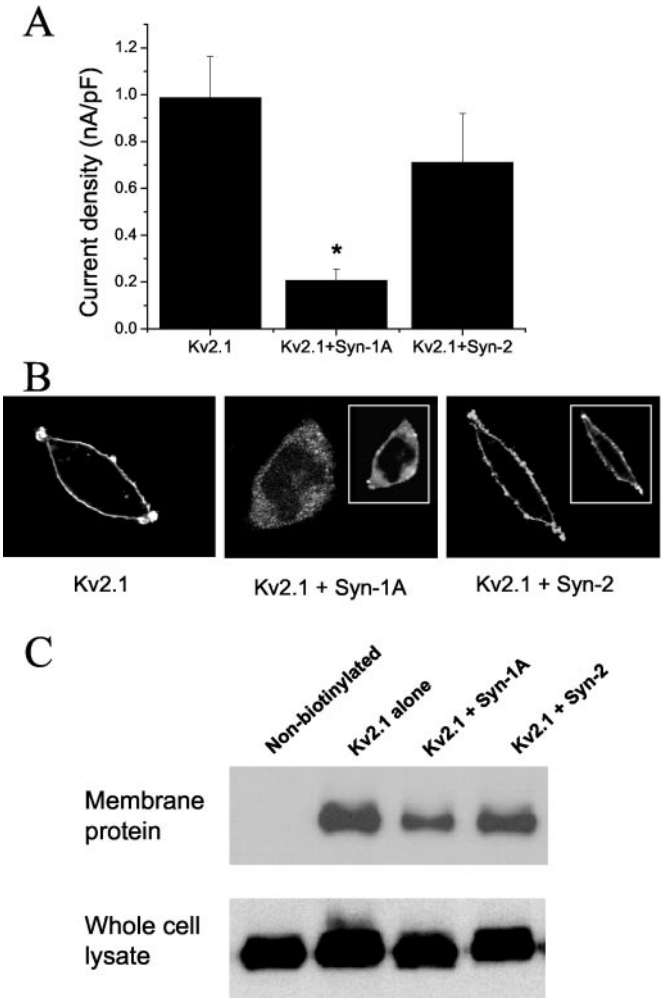

FIG. 4. **Syntaxin 1A reduces Kv2.1 current density by inhibiting the channel surfacing to the plasma membrane.** *A*, Syn-1A reduced Kv2.1 current density. Outward K^+ currents triggered by a +70 mV pulse (250 ms) from a holding potential of −70 mV in HEK293 cells expressing Kv2.1 alone (n = 13), Kv2.1 with Syn-1A (n = 22) or Kv2.1 with Syn-2 (n = 7) were normalized by cell capacitance to yield current density. *, $p < 0.05$ when compared with Kv2.1 alone. *B*, confocal microscopy of Syn-1A inhibition of Kv2.1 surface expression. HEK293 cells were transfected with Kv2.1 in the absence or presence of Syn-1A or -2. Expression of Kv2.1 alone was visualized as a bright and clear FITC fluorescence at the cell periphery (*left panel*). Kv2.1 fluorescence was faint and diffuse with Syn-1A co-expression. *Inset* shows expression of Syn-1A, as visualized by Texas Red fluorescence (*middle panel*). Kv2.1 fluorescence was bright and clear at the cell periphery with Syn-2 co-expression. *Inset* shows expression of Syn-2, as visualized by Texas Red fluorescence (*right panel*). *C*, plasma membrane Kv2.1 protein expression. Transfected HEK293 cells were biotinylated and solubilized as described under "Materials and Methods." Biotinylated proteins (plasma membrane fraction) were isolated using the streptavidin resin. The proteins eluted from the resin (*upper panel*) and whole cell lysates obtained prior to the streptavidin precipitation (*lower panel*) were then separated by PAGE, and the Kv2.1 protein identified by a specific antibody by Western blotting. The whole cell lysate panel is a gross assessment of the effects on Kv2.1 synthesis.

To investigate whether Syn-1A reduced Kv2.1 current density by inhibiting the trafficking of Kv2.1 protein to the plasma membrane, we performed confocal immunofluorescence microscopy (Fig. 4*B*). When Kv2.1 was expressed alone, there was bright and clear fluorescence at the cell periphery, suggesting that the majority of the Kv2.1 channel protein was present at the plasma membrane (Fig. 4*B*, *left panel*). With Syn-1A co-expression, the Kv2.1 plasma membrane fluorescence was dimmer and diffuse (note patches of fluorescence beneath the cell periphery) (Fig. 4*B*, *middle panel*), indicating that the overexpressed Syn-1A (*inset*) inhibited Kv2.1 from surfacing to the plasma membrane, and a substantial proportion of Kv2.1 was retained in the cytoplasm. Consistent with the current density data shown in Fig. 4*A*, overexpression of Syn-2 (*inset*) did not cause significant inhibition of surfacing of Kv2.1 (Fig. 4*B*, *right panel*).

To quantitatively determine the amount of reduction of plasma membrane surfacing of Kv2.1 caused by the overexpression of Syn-1A and Syn-2, we performed the following study. Transfected HEK293 cells were biotinylated so that plasma membrane proteins can be separated from the rest of the cells using the streptavidin resin. Fig. 4*C* (*upper panel*) shows that the levels of plasma membrane Kv2.1 proteins pulled down by the streptavidin resin was reduced by 49% with the Syn-1A co-expression, but only by 22% with the Syn-2 expression. The Kv2.1 proteins in the total lysates obtained just prior to the treatment with streptavidin resin did not change, indicating that both syntaxins did not have any significant effect on total protein synthesis of Kv2.1 (*lower panel*).

Modulation of Kv2.1 Channel Properties by Syn-1A—A number of reports have already shown that SNARE proteins profoundly affected Kv channel electrophysiological properties, such as activation and inactivation kinetics (16, 18, 19). We next explored whether Syn-1A targeted to the plasma membrane by co-expression would modulate the electrophysiological properties of Kv2.1 channel current. Only those cells expressing currents greater than 4 nA were selected for analysis because HEK293 cells express endogenous outward K^+ currents as high as 0.4 nA (data not shown). Kv2.1 had a fairly rapid activation rate, with a τ of 5.6 ± 0.6 ms (Fig. 5*A*). The overexpressed Syn-1A significantly ($p < 0.05$) slowed down the activation rate (τ = 8.5 ± 0.7 ms) while Syn-2 had no effect. Kv2.1 exhibited a very slow inactivation rate (Fig. 5*B*), which was neither affected by Syn-1A nor Syn-2 co-expression.

Since Syn-1A slows down Kv2.1 activation, we then examined whether Syn-1A would affect the voltage dependence of activation of Kv2.1. To study this, instantaneous activation curves were obtained using the protocol in which voltage steps from −50 to +70 mV in 10 mV increments were followed by a −40 mV step to trigger tail currents. Normalized peak tail currents are then plotted against the various voltage steps and fit by the Boltzmann equation (Fig. 6*A*). Syn-1A did not significantly alter the voltage dependence of activation of Kv2.1.

We performed the steady-state inactivation experiments to

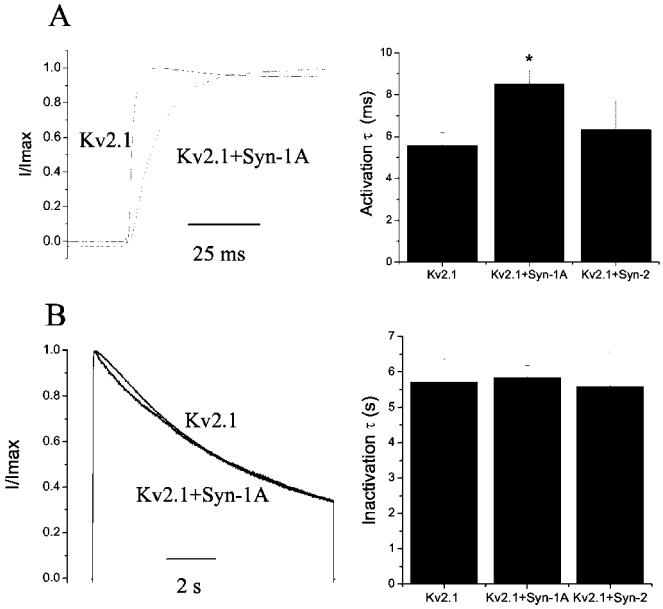

FIG. 5. **Syn-1A slowed Kv2.1 current activation but did not affect current inactivation.** *A*, outward K^+ currents were triggered by a +70 mV pulse (250 ms) from a holding potential of −70 mV in HEK293 cells expressing Kv2.1 with (n = 14) or without Syn-1A (n = 21). Currents shown are normalized to its peak magnitude and overlapped for comparison. Activation time constants were obtained by an exponential fit to the rising phase of the current and were summarized in the graph shown. Syn-1A, but not Syn-2 (n = 7), significantly slowed down activation. *, $p < 0.05$ when compared with Kv2.1 alone. *B*, to show inactivation, outward K^+ currents were triggered by a prolonged +70 mV pulse (10 s) from a holding potential of −70 mV in HEK293 cells expressing Kv2.1 with (n = 5) or without Syn-1A (n = 5). Currents shown are normalized to its peak magnitude and overlapped for comparison. Inactivation time constants were obtained by an exponential fit to the decaying phase of the current, and are summarized in the graph shown. Syn-1A and Syn-2 (n = 7) did not affect the rate of inactivation.

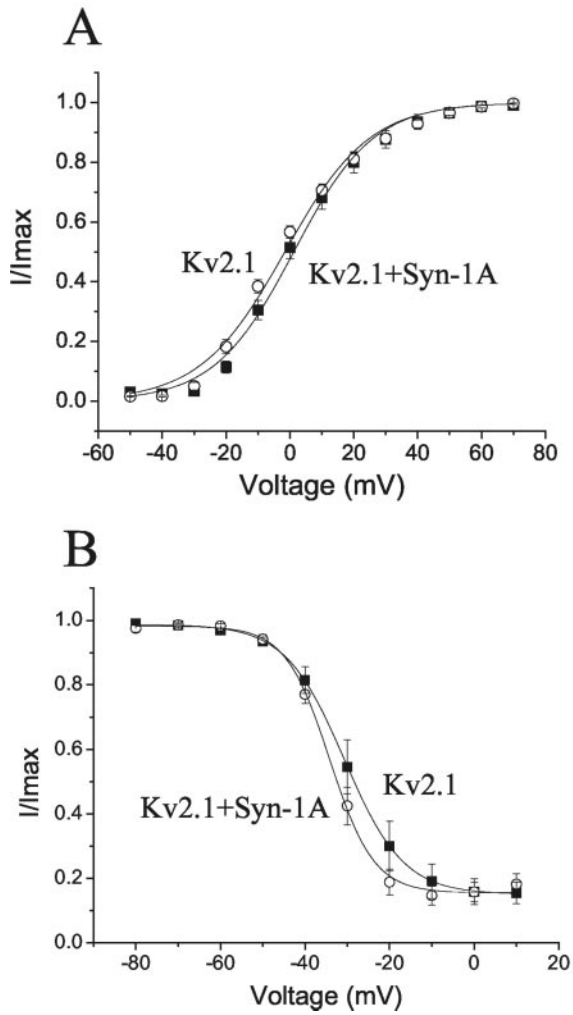

FIG. 6. **Syn-1A did not affect voltage dependence of Kv2.1 current activation but increased the voltage sensitivity of steady-state inactivation in HEK293 cells.** *A*, instantaneous activation curves. Voltage steps from −50 to +70 mV (250 ms) delivered in 10 mV increments from a holding potential of −70 mV were followed by a −40 mV step to trigger tail currents. Normalized peak tail currents are then plotted against the various voltage steps. The curves are best fit by the Boltzmann equation. There is no significant difference between Kv2.1 with (n = 8) and without Syn-1A (n = 10). *B*, steady-state inactivation experiments. A dual-pulse protocol was used in which a test pulse step of +70 mV (largest conductance, see above) was preceded by a long pre-pulse (12 s) of different potentials. The test pulse currents are normalized to the largest test pulse current and plotted against the pre-pulse voltages. The curves are best fit by the Boltzmann equation. There is no significant difference in $V_{1/2}$ between Kv2.1 with (n = 5) and without Syn-1A (n = 7), but Syn-1A significantly decreased the slope factor (see "Results").

determine channel availability for activation as a function of membrane potential. A dual-pulse protocol was used in which a test pulse step of +70 mV was preceded by a long pre-pulse (12 s) of different potentials. The test pulse currents are normalized to the largest test pulse current and plotted against the pre-pulse voltages. The curves are best fit by the Boltzmann equation (Fig. 6*B*). Kv2.1 currents have a half-maximal inactivation potential ($V_{1/2}$) of −29.9 ± 2.5 mV. The left shift of the inactivation curve ($V_{1/2}$ value of −34.7 ± 1.3 mV) caused by Syn-1A was slight and statistically insignificant. However, Syn-1A significantly decreased the slope factor from 6.2 ± 0.63 to 4.4 ± 0.25 ($p < 0.05$), indicating that Syn-1A increased the sensitivity of voltage-dependent inactivation within the physiological range (−40 to −10 mV). Syn-2 did not significantly alter $V_{1/2}$ values and slope factor of inactivation curves (−28.7 ± 2.2 mV and 6.3 ± 0.22, respectively, n = 7).

DISCUSSION

Intensive work in the past decade has revealed the putative interacting domains between VDCC and SNARE proteins (4–8). The secretory vesicle-SNARE protein-Ca^{2+} channel complex ("excitosome") may serve dual purposes. First, it may support very fast secretory response; second, SNARE proteins may provide immediate feedback to the Ca^{2+} channels (4–6). Kv channels provide the repolarizing currents, subsequently causing closure of Ca^{2+} channel and cessation of the release process (10–13). Further regulation of these Kv channels by SNARE proteins would provide an additional feedback mechanism to more tightly regulate the opening and closing of the Ca^{2+} channel, and therefore, the amplitude and duration of exocytosis. Indeed, our recent reports demonstrated that SNAP-25 and Syn-1A directly bind and modulate neuronal Kv1.1 channels at its cytoplasmic N terminus (16, 19). This plasticity, provided by such versatile interactions between these SNARE proteins and Ca^{2+} and Kv channels, is of great importance not only in neurotransmitter release but also in endocrine secretion, particularly the islet β-cell, wherein a more optimal insulin secretion would be able to achieve euglycemia in the treatment of diabetes. Toward the latter, we have recently shown that SNAP-25 binds the N terminus of rat islet β-cell Kv2.1 channels (17). In this work, we have found that Syn-1A also regulates the rat islet β-cell Kv2.1 channel.

We have obtained evidence that Syn-1A modulated rat islet β-cell Kv2.1 channels by binding to a novel domain, the cytoplasmic C terminus. First, dialysis of GST-Syn-1A inhibited the outward currents in rat islet β-cell, which could be blocked by

the cytoplasmic C terminus domain proteins. Second, dialysis of Syn-1A-GST fusion protein into Kv2.1-transfected HEK293 cells caused a similar reduction in current magnitude, which could also be blocked by the Kv2.1 C terminus domain proteins. Third, our GST-Syn-1A was able to specifically pull down the recombinant Kv2.1 cytoplasmic C terminus domain proteins, C1 (412–633) and C2 (634–853), but not GST, and to a much lesser extent, the cytoplasmic N terminus. Peculiarly, despite the slight binding to the Kv2.1 N terminus, dialysis of this peptide fragment had no effect on the inhibitory effect of Syn-1A on Kv2.1 channel activity, in contrast to Kv1.1 channel activity (19). Whereas Syn-1A seems to bind C1 better than C2, C2 was more effective in blocking Syn-1A inhibition of Kv2.1 activity. Our previous reports (16, 17, 19), together with the present study, therefore demonstrate the heterogeneity in the binding of these SNARE proteins with distinct domains (C and N terminus) within the different Kv channel families. This is in contrast to the interactions of these SNARE proteins to a common cytoplasmic domain linking repeats II and III (II-III linker, or the so-called synprint site) with the different families of Ca^{2+} channels (5, 6). We therefore further explored and compared these distinct features of Syn-1A interactions with Kv1.1 and Kv2.1 channels by examining the activation and inactivation kinetics and voltage dependence of activation and steady-state inactivation.

First, in contrast to our previous work showing that Syn-1A co-expression in *Xenopus* oocytes reduced the magnitude of Kv1.1 current, but which did not affect the Kv1.1 current activation rate (18), our current study shows co-expression of Syn-1A substantially slowed down the activation of Kv2.1 current. Both Kv1.1 and Kv2.1 currents exhibit very slow inactivation, which is not affected at all by co-expression of Syn-1A (Ref. 18 and this work). Expression of Kv1.1 together with the Kvβ subunit resulted in a fast inactivation component, and we reported before that Syn-1A could increase the extent of such fast inactivation. In this work, we did not investigate such an effect of Syn-1A, as it has been reported that Kv2.1 does not interact with Kvβ subunits (23).

Because Syn-1A inhibited Kv2.1 currents and slowed down the Kv2.1 current activation, we tested whether Syn-1A would affect the voltage dependence of Kv2.1 activation by analyzing the tail currents. To our surprise, Syn-1A did not cause a significant right shift of the activation curve, indicating that Kv2.1 activated equally readily at lower voltages in the presence of Syn-1A. Thus, Syn-1A appears to have a selective effect on Kv2.1, namely, decelerating activation without affecting its voltage dependence.

Next, we show that Syn-1A can affect the voltage dependence of steady-state inactivation of Kv2.1. Thus, we show that although Syn-1A did not cause significant left shift of the steady-state inactivation curve, it did significantly decrease the slope factor, indicating that Syn-1A enhances the voltage sensitivity of such steady-state inactivation. Remarkably, the slope of the inactivation curves lies within the depolarization ranges, implying that the physiological role of Syn-1A might be to render Kv2.1 channel less available as the cell becomes increasingly depolarized during stimulation. Note that co-expression of Syn-1A has been shown to also modulate steady-state voltage dependence of inactivation of L- and N-type VDCC expressed in *Xenopus* oocytes (24).

We show here that co-expression of Syn-1A reduced Kv2.1 current density. We showed that this is due not only to a direct inhibition of channel activity (Fig. 3), but also to an inhibition of the surfacing of the Kv2.1 protein to the plasma membrane (Fig. 4). The latter was demonstrated by confocal microscopy and at the protein level. We recently showed that Syn-1A has a biphasic effect on Kv1.1 current: low concentration promoting while high concentration reducing current amplitudes (18). The enhancement of current by low syntaxin expression was not accompanied by enhanced expression of channel protein while reduction of current by high syntaxin expression was largely due to a reduced expression. It is noteworthy, however, that SNAP-25 could reduce both Kv1.1 and Kv2.1 current magnitudes without affecting channel surface expression (16, 17). More work is required to determine the mechanism by which Syn-1A regulates Kv channel trafficking to the plasma membrane surface.

We demonstrated recently that insulin release and L-type Ca^{2+} channel activity in HIT-T15 β-cells are suppressed by overexpression of Syn-1A, not Syn-2 (7). We here show that Kv2.1 channels also interact specifically with Syn-1A, but not Syn-2. Syn-1A inhibition of Kv2.1 currents in β-cells implicate the potential physiological significance of such Syn-1A-Kv2.1 interaction in regulating insulin secretion. The interactions between Syn-1A with distinct domains within the different Kv channel families further suggest distinct interacting sites may provide opportunities for Kv channel-specific drug design (15). Kv2.1 is also present in vascular smooth muscle cells and cardiac myocytes (25, 26). Interestingly, we have shown by confocal microscopy that Syn-1A and SNAP-25 are also present in cardiac myocytes and could modify the outward currents.[2] Since myocytes are not actively secreting cells, this suggests the importance of SNARE protein regulation of Kv channels independent of exocytosis. In further support, we had also reported that SNAP-25 modulated Kv and Ca^{2+}-dependent outward K^+ currents in feline esophageal smooth muscle cells (27).

It can be envisaged that during exocytosis SNAP-25, Syn-1A, and Kv2.1 form a complex, reminiscent of the SNARE protein-Ca^{2+} channel complex. Our data here show that, besides reducing current magnitude, Syn-1A has a unique inhibitory profile on Kv2.1 currents: (i) slowing activating without affecting voltage dependence of activation and (ii) increasing sensitivity of voltage dependence of steady-state inactivation without affecting inactivation kinetics. The inhibition of Kv2.1 by Syn-1A may be important in preventing outward K^+ currents during very early β-cell depolarization, but may be modulated or attenuated by SNAP-25 (and perhaps synaptobrevin) during core complex formation. More experiments have to be done to elucidate the dynamics and role of the SNARE protein-Kv channel complex during exocytosis. Our very recent report (19) that G-protein $\beta\gamma$ subunits enhanced Syn-1A binding to Kv1.1/Kvβ and augmented the inactivating effect of Syn-1A on Kv1.1/Kvβ current adds complexity to the regulation of the SNARE protein-Kv1.1 channel complex. Hence, the possibility that additional factors may modulate the functions of the SNARE protein-Kv2.1 channel complex awaits exploration.

REFERENCES

1. Gerber, S. H., and Sudhof, T. C. (2002) *Diabetes* **51,** Suppl. 1**,** S3–S11
2. Rizo, J., and Sudhof, T. C. (2002) *Nat. Rev. Neurosci.* **3,** 641–653
3. Rettig, J., and Neher, E. (2002) *Science* **298,** 781–785
4. Seagar, M., and Takahashi, M. (1998) *J. Bioenerg. Biomembr.* **30,** 347–356
5. Catterall, W. A. (1999) *Ann. N. Y. Acad. Sci.* **868,** 144–159
6. Atlas, D. (2001) *J. Neurochem.* **77,** 972–985
7. Kang, Y., Huang, X., Pasyk, E. A., Ji, J., Holz, G. G., Wheeler, M. B., Tsushima, R. G., and Gaisano, H. Y. (2002) *Diabetologia* **45,** 231–241
8. Ji, J., Yang, S. N., Huang, X., Li, X., Sheu, L., Diamant, N., Berggren, P. O., and Gaisano, H. Y. (2002) *Diabetes* **51,** 1425–1436
9. Nichols, C. G., and Koster, J. C. (2002) *Am. J. Physiol.* **283,** E403–E412
10. Hille, B. (1992) *Ionic Channels in Excitable Membranes*, 2nd Ed., pp. 115–139, Sinauer Associates, Sunderland, MA
11. Yellen, G. (2002) *Nature* **419,** 35–42
12. Smith, P. A., Bokvist, K., Arkhammar, P., Berggren, P. O., and Rorsman, P. (1990) *J. Gen. Physiol.* **95,** 1041–1059

[2] H. Y. Gaisano and R. G. Tsushima, unpublished data.

13. Roe, M. W., Worley, J. F. 3rd, Mittal, A. A., Kuznetsov, A., DasGupta, S., Mertz, R. J., Witherspoon, S. M. 3rd, Blair, N., Lancaster, M. E., McIntyre, M. S., Shehee, W. R., Dukes, I. D., and Philipson, L. H. (1996) *J. Biol. Chem.* **271,** 32241–32246
14. Henquin, J. C., Meissner, H. P., and Preissler, M. (1979) *Biochim. Biophys. Acta* **587,** 579–592
15. MacDonald, P. E., Sewing, S., Wang, J., Joseph, J. W., Smukler, S. R., Sakellaropoulos, G., Wang, J., Saleh, M. C., Chan, C. B., Tsushima, R. G., Salapatek, A. M., and Wheeler, M. B. (2002) *J. Biol. Chem.* **277,** 44938–44945
16. Ji, J., Tsuk, S., Salapatek, A. M., Huang, X., Chikvashvili, D., Pasyk, E. A., Kang, Y., Sheu, L., Tsushima, R., Diamant, N., Trimble, W. S., Lotan, I., and Gaisano, H. Y. (2002) *J. Biol. Chem.* **277,** 20195–20204
17. MacDonald, P. E., Wang, G., Tsuk, S., Dodo, C., Kang, Y., Tang, L., Wheeler, M. B., Cattral, M. S., Lakey, J. R., Salapatek, A. M., Lotan, I., and Gaisano, H. Y. (2002) *Mol. Endocrinol.* **16,** 2452–2461
18. Fili, O., Michaelevski, I., Bledi, Y., Chikvashvili, D., Singer-Lahat, D., Boshwitz, H., Linial, M., and Lotan, I. (2001) *J. Neurosci.* **21,** 1964–1974
19. Michaelevski, I., Chikvashvili, D., Tsuk, S., Fili, O., Lohse, M. J., Singer-Lahat, D., and Lotan, I. (2002) *J. Biol. Chem.* **277,** 34909–34917
20. Hamill, O. P., Marty, A., Neher, E., Sakmann, B., and Sigworth, F. J. (1981) *Pflugers Arch.* **391,** 85–100
21. MacDonald, P. E., Ha, X. F., Wang, J., Smukler, S. R., Sun, A. M., Gaisano, H. Y., Salapatek, A. M., Backx, P. H., and Wheeler, M. B. (2001) *Mol. Endocrinol.* **15,** 1423–1435
22. Jarvis, S. E., and Zamponi, G. W. (2001) *J. Neurosci.* **21,** 2939–2948
23. Rhodes, K. J., Strassle, B. W., Monaghan, M. M., Bekele-Arcuri, Z., Matos, M. F., and Trimmer, J. S. (1997) *J. Neurosci.* **17,** 8246–8258
24. Wiser, O., Bennett, M. K., and Atlas, D. (1996) *EMBO J.* **15,** 4100–4110
25. Xu, C., Lu, Y., Tang, G., and Wang, R. (1999) *Am. J. Physiol.* **277,** G1055–G1063
26. Schultz, J. H., Volk, T., and Ehmke, H. (2001) *Circ. Res.* **88,** 483–490
27. Ji, J., Salapatek, A. M., Lau, H., Wang, G., Gaisano, H. Y., and Diamant, N. E. (2002) *Gastroenterology* **122,** 994–1006